JPE 16-4-3

http://dx.doi.org/10.6113/JPE.2016.16.4.1268
ISSN(Print): 1598-2092 / ISSN(Online): 2093-4718

Long-Lasting and Highly Efficient TRIAC Dimming LED Driver with a Variable Switched Capacitor

Eun-Soo Lee[*], Bo-Hwan Choi[*], Duy Tan Nguyen[*], Byeung-Guk Choi[*], and Chun-Taek Rim[†]

[*,†]Department of Nuclear and Quantum Engineering, KAIST, Daejeon, Korea

Abstract

A triode for alternating current (TRIAC) dimming light emitting diode (LED) driver, which adopts a variable switched capacitor for LED dimming and LED power regulation, is proposed in this paper. The proposed LED driver is power efficient, reliable, and long lasting because of the TRIAC switch that serves as its main switch. Similar to previous TRIAC dimmers for lamps, turn-on timing of a TRIAC switch can be controlled by a volume resistor, which modulates the equivalent capacitance of the proposed variable switched capacitor. Thus, LED power regulation against source voltage variation and LED dimming control can be achieved by the proposed LED driver while meeting the global standards for power factor (PF) and total harmonic distortion (THD). The long life and high power efficiency of the proposed LED driver make it appropriate for industrial lighting applications, such as those for streets, factories, parking garages, and emergency stairs. The detailed analysis of the proposed LED driver and its design procedure are presented in this paper. A prototype of 80 W was fabricated and verified by experiments, which showed that the efficiency, PF, and THD at V_s = 220 V are 93.8%, 0.95, and 22.5%, respectively; 65 W of LED dimming control was achieved with the volume resistor, and the LED power variation was well mitigated below 3.75% for 190 V < V_s < 250 V.

Key words: Industrial lighting applications, LED dimming, LED power regulation, Long-life characteristic, TRIAC dimming control, Variable switched capacitor

I. INTRODUCTION

Conventional lamps such as fluorescent lamps and incandescent lamps are being replaced with light emitting diode (LED) lamps due to their high efficacy and long life [1]-[6]. LED drivers provide LED lamps with controlled or regulated current regardless of source voltage or temperature variations. Switched-mode-power-supply (SMPS) LED drivers are most widely used because of their compact size, high power factor (PF), and low total harmonic distortion (THD) [7]-[24]. However, these LED drivers may suffer from switching loss and a relatively short operating life in comparison with LED lamps. These drawbacks reduce the total lifetime of LED lighting systems composed of LED lamps and dedicated LED drivers. Hence, passive LED drivers are preferred because of their extremely high power efficiency and long life [25]-[29]. Even though switching devices such as MOSFET and BJT are not adopted in the LED drivers, the PF and THD characteristics can be satisfied with global standards with a simple structure. However, one of the major drawbacks of passive LED drivers in LED lamps is their lack of a current regulation capability for source voltage variation. This shortcoming hinders the commercialization of such LED drivers.

In order to provide LED power regulation capability with high efficiency and long-life characteristics, a triode for alternating current (TRIAC) dimming control LED driver with a passive input filter was proposed [30], [31]. This LED driver adopts a variable switched capacitor to modulate LED power, which can be controlled through the turn-on duration of a TRIAC together with a diode for alternating current (DIAC); in this way, it was proven that LED dimming and LED power regulation are successfully achieved. Due to the bulky size of two inductors and many capacitors in a passive input filter, however, the total size of this LED driver becomes large, and efficiency is as low as 92%; hence, this LED driver may not be a good candidate for practical lighting solutions. Furthermore, a complicated passive input filter, which is composed of two inductors and five capacitors,

Manuscript received Nov. 16, 2015; accepted Feb. 19, 2016
Recommended for publication by Associate Editor Chun-An Cheng.
[†]Corresponding Author: ctrim@kaist.ac.kr
Tel: +82-42-350-3827, Fax: +82-42-350-3861, KAIST
[*]Department of Nuclear and Quantum Eng., KAIST, Korea

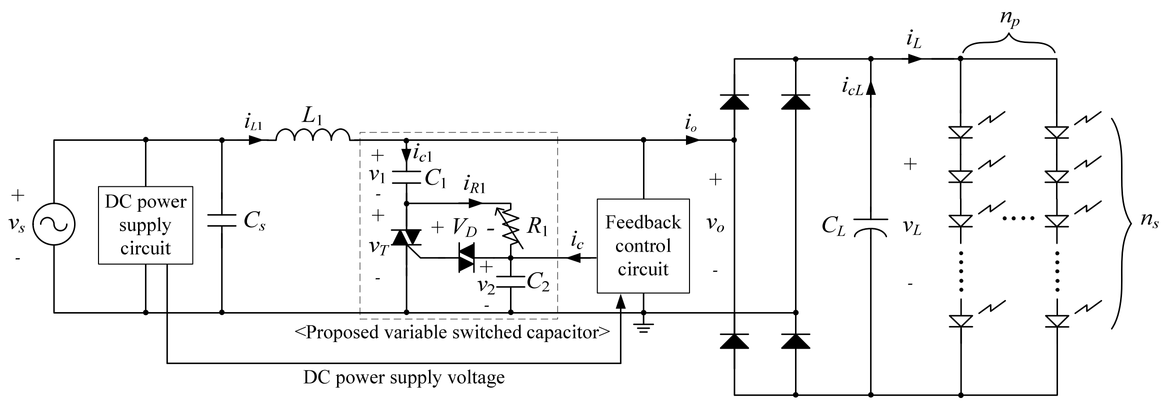

Fig. 1. Overall circuit configuration of the proposed TRIAC dimming LED driver.

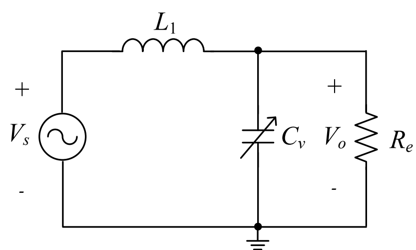

Fig. 2. The equivalent circuit of the proposed LED driver.

makes this LED circuit almost impossible to be analyzed due to its high-order system.

In this paper, a TRIAC dimming LED driver, which reduces the number of passive components in the passive input filter and improves power efficiency in comparison with the aforementioned TRIAC dimming control LED driver [30]-[31], is proposed, as shown in Fig. 1. Only one inductor L_1 and two capacitors C_1 and C_2 with a TRIAC, DIAC, and volume resistor are adopted for the passive input filter and the variable switched capacitor [32], which makes this LED circuit simple, compact, and possible to analyze. The detail operating principle of the proposed variable switched capacitor, design procedure, and additional simulation and experimental results, which were not described in [32] in detail, are additionally provided in this paper. It shows successful LED dimming and LED power regulation capabilities, meeting the PF and THD standards over a wide range of source voltages.

II. Static Analysis of the Proposed LED Driver

A. Operating Principle of the Proposed LED Driver

The proposed LED driver, as shown in Fig. 1, is based on the previous TRIAC dimming LED driver [30], [31]; hence, except for a passive input filter and a variable switched capacitor, the other circuit components such as a DC power supply circuit and a feedback control circuit are the same as previous one. In order to provide this LED driver with an LED power control function, a conventional TRIAC switch with a DIAC is inserted in series with C_1 to vary the connecting time portion of C_1 in a switching period, which results in a variation of equivalent capacitance for the proposed variable switched capacitor. Note that n_s and n_p are the number of LEDs in series and parallel, respectively, and C_s is used only for the PF compensation.

As shown in Fig. 2, the equivalent circuit of the proposed LED driver can be obtained, by regarding the switched capacitor circuit of C_1, C_2, and R_1 with a TRIAC and DIAC as an equivalent variable capacitor C_v, and by simplifying the diode rectifier and DC load circuit as an equivalent resistor R_e [33]-[34]. Note that high-order switching harmonics are neglected, and only the fundamental components of voltage and current are considered. The DC voltage gain G_V, which is the ratio of output voltage V_o and source voltage V_s, is then determined as follows:

$$G_V \equiv \left|\frac{V_o}{V_s}\right| = \frac{R_e}{\sqrt{R_e^2(1-\omega_s^2 L_1 C_v)^2 + \omega_s^2 L_1^2}} = G_V(C_v) \quad , \tag{1}$$

$$R_e \cong \alpha^2 R_L \quad (\because R_L \equiv \frac{V_L}{I_L}) \quad , \tag{2}$$

where α is a DC-AC voltage conversion ratio when a bridge diode is converted to an equivalent auto-transformer [35]-[38].

As identified from (1), G_V increases when C_v increases as long as the source angular frequency ω_s is less than the resonant angular frequency ω_r, which is exactly the case in the proposed design, as follows:

$$\omega_s < \omega_r, \quad \because \omega_r = \frac{1}{\sqrt{L_1 C_v}} \quad . \tag{3}$$

Therefore, the LED power, corresponding to V_o, can be appropriately controlled by C_v.

B. Operating Mode Analysis of the Proposed Led Driver

The operating mode of the proposed LED driver can be classified into four modes, as shown in Figs 3-4, where each mode will be described in detail in this section. The LED lamps can be replaced with a dynamic resistance r_d and a DC

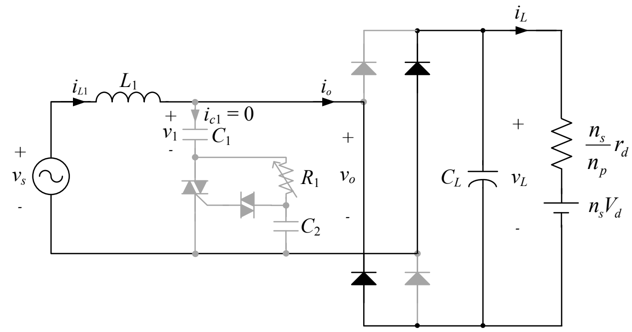

(a) Mode 1.

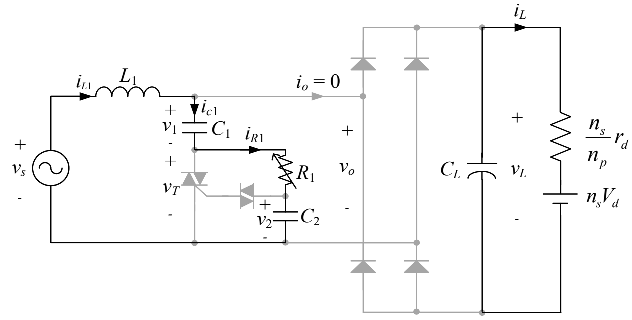

(b) Mode 2.

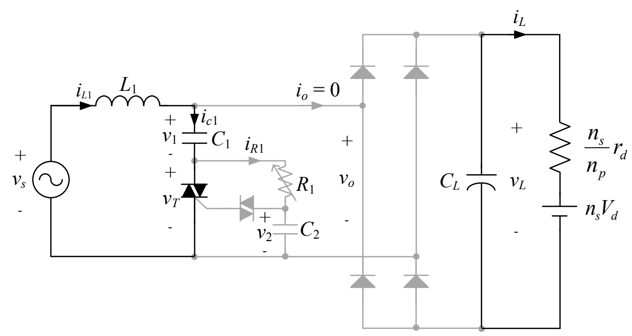

(c) Mode 3.

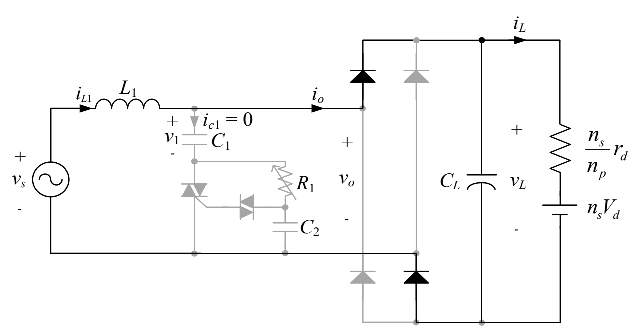

(d) Mode 4.

Fig. 3. Operating modes of the proposed LED driver.

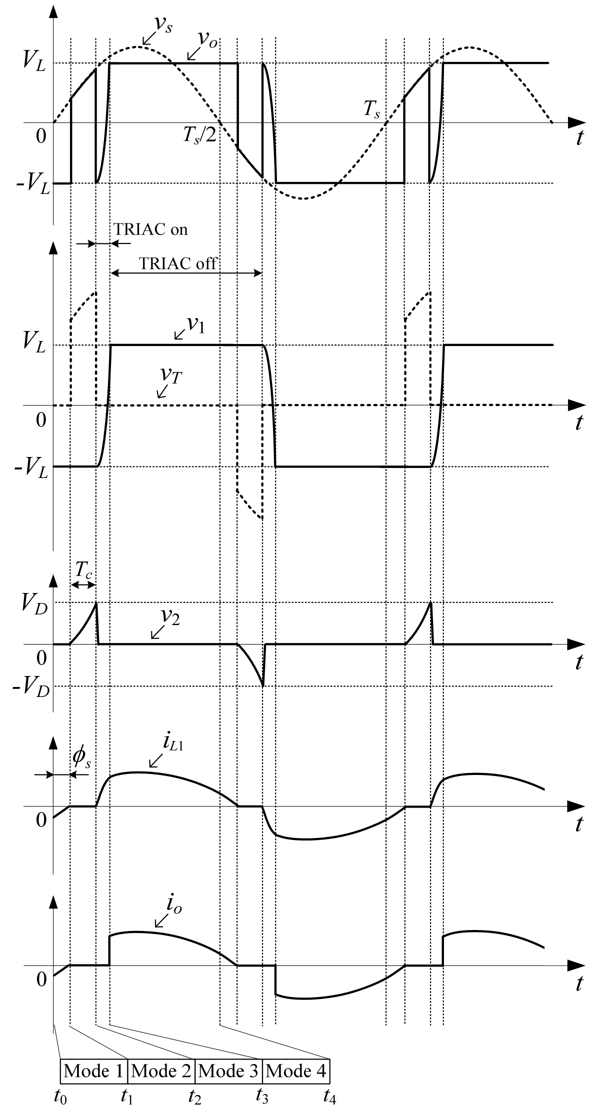

Fig. 4. Waveform diagrams of the proposed LED driver.

voltage source V_d at a specific operating point of the LED current [29]-[31]. The internal resistance of L_1 and the other equivalent series resistances (ESRs) of the capacitors, a TRIAC, a DIAC, and diodes in a diode rectifier are omitted from consideration throughout this paper for simplicity of analysis. The characteristics of all the LED lamps are assumed to be identical, and the temperature distribution over the LED lamps is assumed to be even. All the circuit parameters are assumed to be ideal unless otherwise specified.

Mode 1 [t_0, t_1] : As shown in Fig. 4, the phase difference between V_s and V_o ϕ_s should be defined to identify the beginning of the charging time for C_2 t_1. The detailed procedure to derive ϕ_s has been explained for a passive-type LC^3 LED driver [29], except for a parallel resonance capacitor, which is not connected to the inductor L_1 in parallel in the proposed LED driver.

Mode 2 [t_1, t_2] : In this mode, the TRIAC is turned off and the initial condition is $v_2(t_1) = 0$. After t_1, the charging of v_2 through L_1, C_1, and R_1 is initiated until v_2 reaches the DIAC voltage V_D. Given the negative charge of v_1 from the previous negative polarity operation of v_s, v_1 is approximately $-V_L$ in this mode. R_1 is so largely chosen, i.e., R_1 = 1 MΩ, in this paper; hence, it is assumed that DC voltage v_1 and AC voltage v_s are applied to R_1. Then, the current of R_1 i_{R1} can be determined as follows:

$$i_{R1}(t) \cong \frac{v_s(t)-v_1(t)}{R_1} = \frac{V_s \sin\omega_s t + V_L}{R_1} \quad . \qquad (4)$$

Therefore, v_2 can be determined as follows:

$$\begin{aligned} v_2(t) &\equiv \frac{1}{C_2}\int_{t_1}^{t} i_{c2}(t)dt = \frac{1}{C_2}\int_{t_1}^{t} i_{R1}(t)dt \\ &= \frac{V_s}{\omega_s C_2 R_1}(\cos\omega_s t_1 - \cos\omega_s t) + \frac{V_L}{C_2 R_1}(t-t_1) \end{aligned} \quad . \qquad (5)$$

From (5), the end of the charging time for v_2, i.e. t_2, can be identified when $v_2(t_2) = V_D$.

Mode 3 [t_2, t_3] : In this mode, the TRIAC is turned on and the initial conditions are $v_1(t_2) = v_o(t_2) = -V_L$, $i_{L1}(t_2) = 0$, and $i_o(t_2) = 0$. Thereafter, the proposed LED circuit becomes an LC series resonant circuit, which is composed of L_1 and C_1, as shown in Fig. 3(c). Then, v_1 can be determined as follows:

$$\begin{aligned} v_1(t) &= \frac{1}{(\omega_s^2-\omega_o^2)}\{A\cos\omega_o(t-t_2) + B\sin\omega_o(t-t_2)\} \\ &+ \left(\frac{\omega_o}{\omega_s}\right)^2 \frac{1}{(\omega_s^2-\omega_o^2)}\{C\cos\omega_s(t-t_2) + D\sin\omega_s(t-t_2)\} \end{aligned} \qquad (6a)$$

$$\because A = (V_s \sin\omega_s t_2 + V_L)\omega_o^2 - V_L\omega_s^2, \quad B = V_s\omega_s\omega_o\cos\omega_s t_2, \qquad (6b)$$

$$C = -(V_s\sin\omega_s t_2 + V_L)\omega_s^2 + V_L\omega_s^2, \quad D = -V_s\omega_s^2\cos\omega_s t_2, \qquad (6c)$$

$$\omega_o = \frac{1}{\sqrt{L_1 C_1}} \quad . \qquad (6d)$$

From (6), i_{L1} can be determined as follows:

$$\begin{aligned} i_{L1}(t) &= \frac{1}{L_1}\int_{t_2}^{t}\{v_s(t)-v_1(t)\}dt = \frac{V_s}{\omega_s L_1}(\cos\omega_s t_2 - \cos\omega_s t) \\ &- \frac{1}{L_1(\omega_s^2-\omega_o^2)}\left[\frac{A}{\omega_o}\sin\omega_o(t-t_2) + \frac{B}{\omega_o}\{1-\cos\omega_o(t-t_2)\}\right] \\ &- \left(\frac{\omega_o}{\omega_s}\right)^2 \frac{1}{L_1(\omega_s^2-\omega_o^2)}\left[\frac{C}{\omega_s}\sin\omega_s(t-t_2) + \frac{D}{\omega_s}\{1-\cos\omega_s(t-t_2)\}\right] \end{aligned} \quad . \qquad (7)$$

From (6a), the end of this mode can be determined when $v_1(t_3) = V_L$.

Mode 4 [t_3, t_4] : In this mode, the TRIAC is turned off. The diode rectifier is conducted, which results in $v_1(t) = v_o(t) = V_L$; hence, i_{L1} can be determined as follows:

$$\begin{aligned} & L_1\frac{di_{L1}(t)}{dt} = V_s\sin\omega_s t - V_L \\ & \rightarrow \therefore i_{L1}(t) = \frac{V_s}{\omega_s L_1}(\cos\omega_s t_3 - \cos\omega_s t) - \frac{V_L}{L_1}(t-t_3) + i_{L1}(t_3) \end{aligned} \quad . \qquad (8)$$

From (8), i_{L1} and i_o in this mode are the same as those in Mode 1, except for the polarity. This mode ends when $v_s(t_4) = 0$.

C. Variable Switched Capacitor

The equivalent capacitance of the proposed variable switched capacitor in Fig. 1 can be controlled by modulating the control time T_c, as identified from Figs 3-4. T_c can be modulated by changing the volume resistor R_1 and be determined from (5).

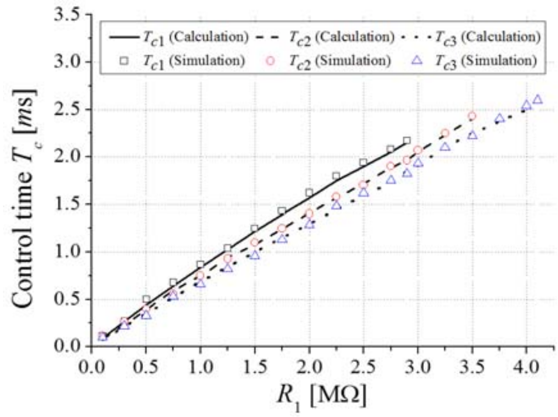

Fig. 5. Calculation and simulation results of control time T_c w.r.t. R_1.

To confirm the modulation of T_c by R_1, a PSIM simulation is performed for the circuit of Fig. 1 without a feedback control circuit and a DC power supply circuit. The parameter values of Fig. 1 are as follows: L_1 = 1.03 H, C_1 = 2.0 μF, C_2 = 10 nF, V_D = 32 V, C_L = 100 μF, n_s = 85, and n_p = 4; then, V_L = 235 V is determined with the assumption that V_d and r_d are 2.7 V and 3.5 Ω, respectively, at the nominal LED current of 80 mA [29]. As shown in Fig. 5, the simulation results are in good agreement with the theoretical analysis of (5), where T_{c1}, T_{c2}, and T_{c3} are the control times for V_s = 190 V, 220 V, 250 V, respectively. The R_1 values greater than 2.9, 3.5, and 4.1 MΩ for T_{c1}, T_{c2}, and T_{c3}, respectively, cannot be adopted in Fig. 5 because v_2 in Fig. 4 cannot reach V_D as a result of the slow charging time of T_c given a large R_1.

It is possible to find out an equivalent variable capacitance C_v with respect to T_c determined by R_1, as identified from Fig. 5; hence, the C_v is found by comparing the LED power of the proposed LED driver with that of a LED circuit with only C_1 in the proposed variable switched capacitor of Fig. 1. From Fig. 6, it is found that the equivalent capacitance can be appropriately controlled by R_1 from the simulation results, where C_{v1}, C_{v2}, and C_{v3} are the equivalent variable capacitances for V_s = 190 V, 220 V, 250 V, respectively. In Fig. 6, a load resistor R_L is connected to the load for a general static analysis of the proposed variable switched capacitor. The value of R_L is set to 734 Ω with consideration of V_L = 235 V and I_L = 0.32 A in (2): an R_1 value greater than 1.9, 2.3, and 2.8 MΩ for C_{v1}, C_{v2}, and C_{v3}, respectively, cannot be adopted in this case. From the simulation results of Fig. 6, calculation and simulation results of normalized V_L are shown in Fig. 7, where V_{L1}, V_{L2}, and V_{L3} are the normalized load voltages for V_s = 190 V, 220 V, 250 V, respectively. From (1)-(2), V_L ($\equiv V_o/\alpha$) can be calculated and α is assumed to be 0.8 for a non-linear diode rectifier [29]. Therefore, it is found from Fig. 7 that the proposed variable switched capacitor can modulate

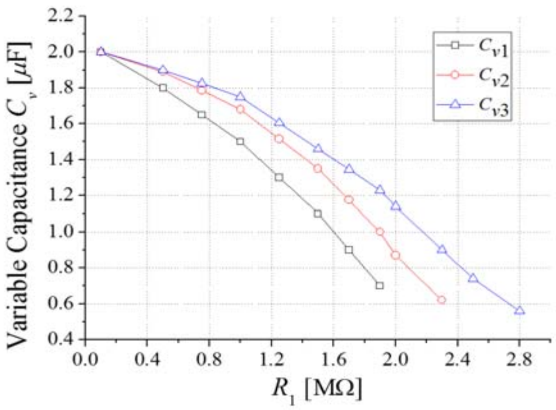

Fig. 6. Simulation results of the variable switched capacitance C_v w.r.t. R_1.

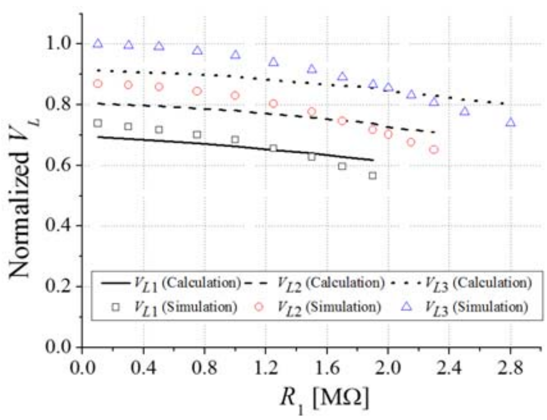

Fig. 7. Calculation and simulation results of normalized V_L w.r.t. R_1.

TABLE I
CIRCUIT PARAMETERS OF THE PROPOSED LED DRIVER

Parameters	Values	Parameters	Values
L_1	1.03 H	R_1	1 MΩ
C_1	2.0 μF	n_s	85
C_2	10 nF	n_p	4
C_s	2.68 μF	TRIAC	2N6075AG
C_L	100 μF	DIAC	DB3

load voltage for LED dimming and power regulation.

III. DESIGN OF THE PROPOSED LED DRIVER

As shown in Fig. 1, the proposed LED driver was based on the passive-type LC^3 LED driver [29]; hence, circuit parameters for 80 W of power were chosen in a similar way, as listed in Table I.

With regard to the proposed variable switched capacitor in Fig. 1, a small value of C_2 and a large value of R_1 are recommended to reduce the size of C_2 and the power loss in R_1; hence, C_2 and R_1 are set to 10 nF and 1.0 MΩ, respectively. The worst case for power dissipation in R_1 is roughly $(2V_L)^2/R_1 \cong (2\cdot 235)^2/1\text{M} \cong 221\,m\text{W}$, which is below 1/4 W. C_1 is selected as 2.0 μF, considering the range of the variable switched capacitance. The breakover voltage V_D for the DIAC is set to 32 V, considering commercial availability of the DIAC. The component for the TRIAC was a 2N6075AG with a 600 V voltage rating and a 4 A current rating. The load capacitor C_L, which reduces the flickering of LED lamps, is set to 100 μF to satisfy the recent international standard, i.e., IEEE 1789-2015 [39]; hence, the maximum percent flicker of the proposed LED driver when R_1 = 3.5MΩ and V_s = 250V, as identified from Figs. 4-5, is calculated as 6.38%, which is less than 10% of the international standards. The PF compensation capacitor C_s is 2.68 μF to satisfy the PF regulation [40].

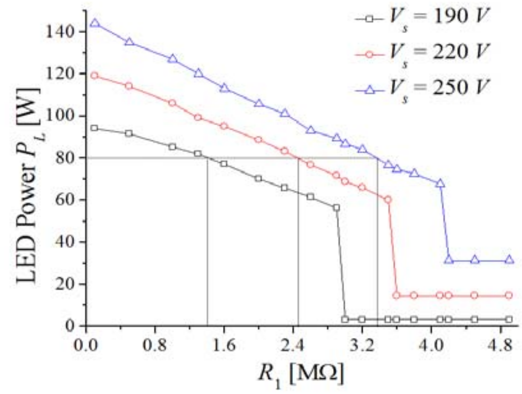

Fig. 8. Simulation results of LED power w.r.t. R_1.

To confirm LED dimming by the volume resistor R_1, a PSIM simulation is performed without a feedback control circuit and a DC power supply circuit, as shown in Fig. 8. The internal resistance of inductor, which is 13 Ω for the prototype of the proposed LED driver in Fig. 9, and the other parasitic components are not considered in the simulation verifications. As R_1 increases, T_c increases, and the equivalent capacitance of C_v decreases, which results in the decrease in LED power, as identified from Figs. 5-7. In this way, the LED dimming by the volume resistor is achievable for a wide range of source voltages, like a conventional TRIAC dimmer [18]. For a constant LED power P_L = 80 W, R_1 should be appropriately varied between 1.3 and 3.4 MΩ for a source voltage of 190 V < V_s < 250 V, which is a ± 30 V variation in the rated source voltage of 220 V. Under constant source voltage of V_s = 220 V, LED dimming is achieved with the volume resistor from 120 W to 60 W by the volume resistor.

IV. EXPERIMENTAL VERIFICATIONS

As shown in Fig. 9, a prototype of the proposed LED driver for 80 W LED power was fabricated, as listed in Table I. The other circuit parameters of the DC power supply circuit and feedback control circuit, as shown in Fig. 1, can be determined by a design procedure [30], [31]. The proposed

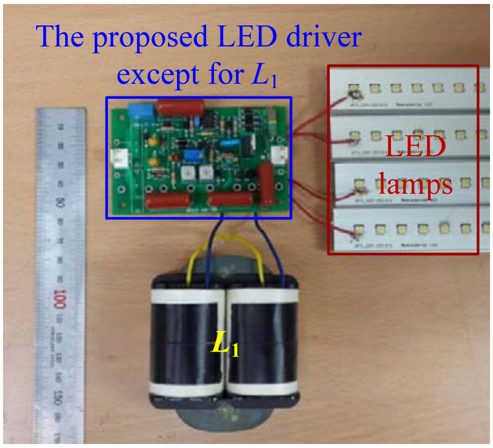

Fig. 9. Prototype of the proposed LED driver.

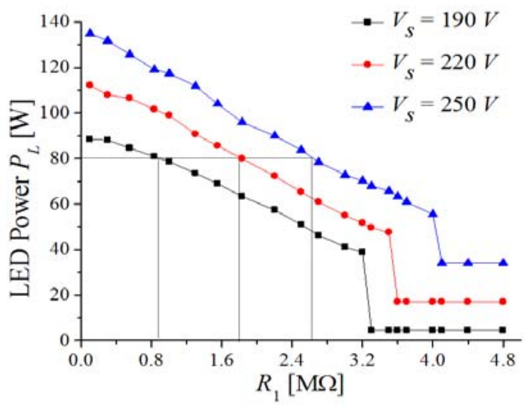

Fig. 10. Experimental results of LED power w.r.t. R_1.

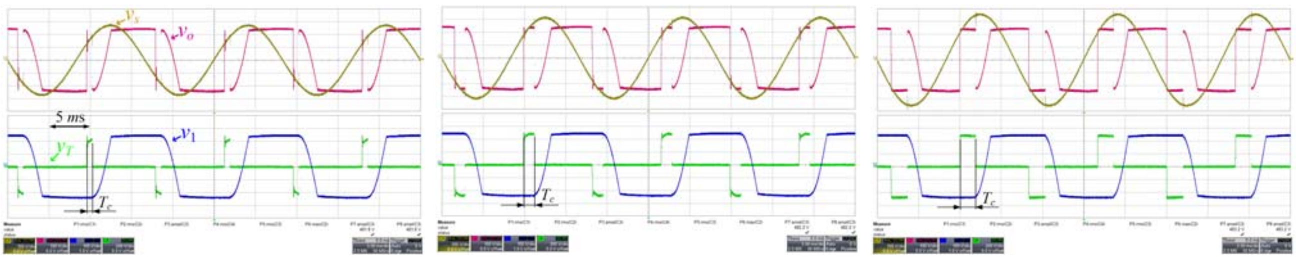

(a) V_s = 190 V. (b) V_s = 220 V. (c) V_s = 250 V.

Fig. 11. Experimental waveforms of v_s, v_o, v_1, and v_T for V_s = 190 V, 220 V, and 250 V at f_s = 60 Hz.

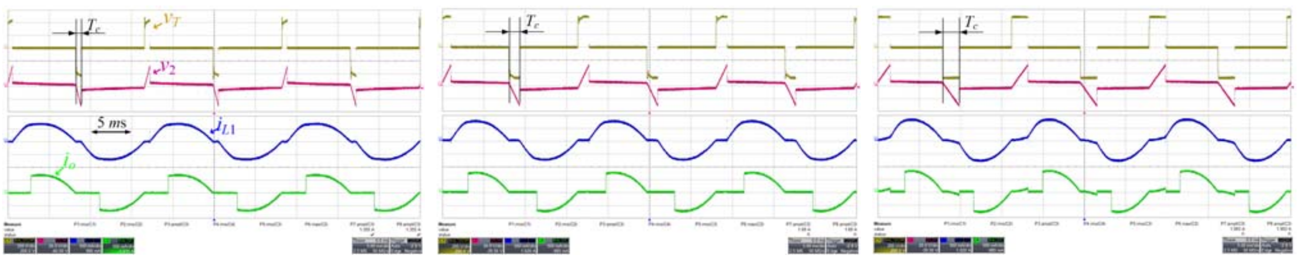

(a) V_s = 190 V. (b) V_s = 220 V. (c) V_s = 250 V.

Fig. 12. Experimental waveforms of v_T, v_2, i_{L1}, and i_o for V_s = 190 V, 220 V, and 250 V at f_s = 60 Hz.

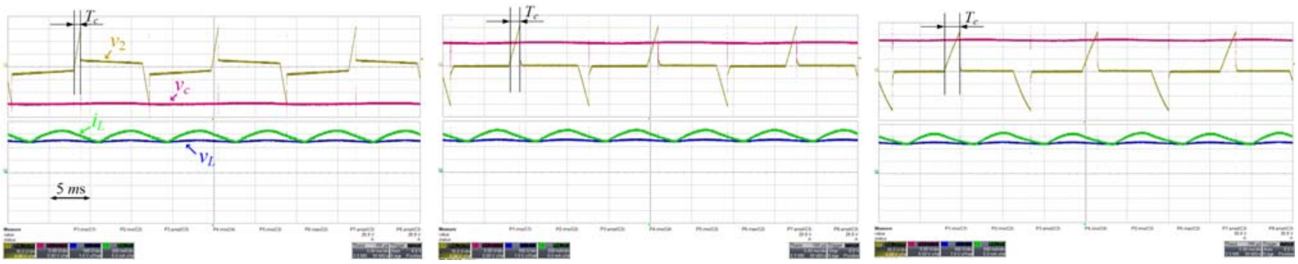

(a) V_s = 190 V. (b) V_s = 220 V. (c) V_s = 250 V.

Fig. 13. Experimental waveforms of v_2, v_c, i_L, and v_L for V_s = 190 V, 220 V, and 250 V at f_s = 60 Hz.

LED driver can be used for high LED power applications that require a power level of as high as 80–100 W. Thus, a slightly large inductor L_1 is of no practical concern because of the large accommodation space for industrial lighting applications, which usually require highly efficient and long-lasting LED drivers. An inductor L_1 in Fig. 9 was fabricated with a silicon steel plate core, and the parasitic resistance of the fabricated inductor L_1 was measured as 13.0 Ω. The current rating of the fabricated inductor was 550 *m*A, and the total weight of the prototype LED driver was measured as 960 g. The inductor L_1 and proposed LED driver weighed 930 and 30 g, respectively; hence, the proposed LED driver is lighter and smaller than conventional TRIAC dimming LED drivers weighing 1,390 g [30], [31].

A. LED Dimming

As shown in Fig. 10, the LED dimming of the proposed LED driver without a feedback control circuit [30]-[31] was

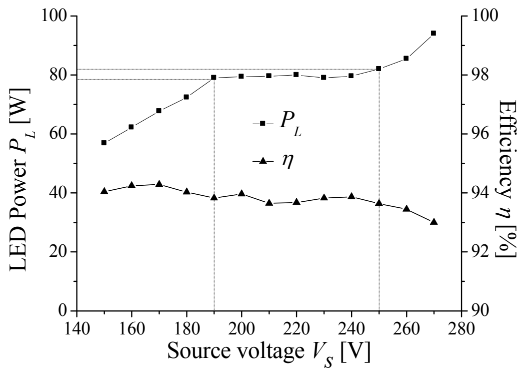

Fig. 14. Experimental results of P_L and η.

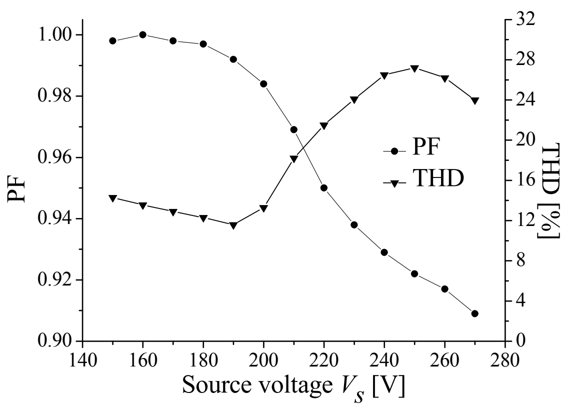

Fig. 15. Experimental results of PF and THD.

experimentally verified. The LED power can be controlled by appropriately modulating the volume resistor R_1. For example, LED power can be changed from 112 W to 47 W at V_s = 220 V, which matches well with the simulation results in Fig. 9.

As shown in Fig. 10, R_1 can be set to satisfy P_L = 80 W for each source voltage: R_1 = 0.83 MΩ, 1.83 MΩ, and 2.6 MΩ for V_s = 190 V, 220 V, and 250 V, respectively. On the basis of these values, the experimental waveforms of v_s, v_o, v_1, v_T, v_2, i_{L1}, and i_o were measured, as shown in Figs. 11 and 12, where T_c increased as R_1 increased, as anticipated from Fig. 5; T_c was measured as 0.63 *m*s, 1.21 *m*s, and 1.90 *m*s for V_s = 190 V, 220 V, and 250 V, respectively, whose values are in good agreements with the calculation and simulation results in Fig. 5.

B. LED Power Regulation, PF, and THD

The experimental waveforms of v_2, v_c, i_L, and v_L were measured, as shown in Fig. 13, where v_c is the control voltage of a current mirror in the feedback control circuit [30], [31]. Obviously, v_c increased when v_s increased to control the charging time of C_2; specifically, V_c was measured as -15 V, 8.9 V, and 12.8 V for V_s = 190 V, 220 V, and 250 V, respectively. As a result, load voltage V_L and current I_L in Fig. 13 were successfully regulated against a wide range of variations in source voltage.

The experimental results of LED power regulation and power efficiency with respect to the source voltage are shown in Fig. 14. The LED power regulation can be implemented by the feedback control circuit [30]-[31]. The LED power variation was mitigated below 3 W for 190 V < V_s < 250 V, with such variation negligible in terms of the change in light brightness. The power efficiency was measured from 93.6% to 94.0% for 190 V < V_s < 250 V, such range is greater than the power efficiency range of conventional LED drivers [13]-[23], [30]-[31]. Over 80% of all the power losses originated from the conduction loss in the fabricated inductor L_1; hence, a higher efficiency than that of the previous LED driver was achieved [30]-[31], and such efficiency can be further improved if the internal resistance of L_1 is reduced. The other losses included conduction losses of the diode rectifier and volume resistor, BJTs and op-amps in the feedback control circuit, and other ESRs. As shown in Fig. 15, the measured results of PF and THD also satisfy the global standards for 190 V < V_s < 250 V [40]-[41] and are superior to those of conventional LED drivers [13], [20]-[23]. All the measurement results for different source voltages are summarized in Table II.

TABLE II
SUMMARY OF EXPERIMENTAL RESULTS FOR SOURCE VOLTAGE VARIATION (190 V < V_S < 250 V)

Measured parameters	Source voltage (V_s)		
	190 V_{rms}	220 V_{rms}	250 V_{rms}
P_s	83.9 W	85.6 W	87.5 W
P_L	78.9 W	80.3 W	81.9 W
PF	0.992	0.950	0.922
THD	12.6%	22.5%	27.0%
Power efficiency	94.0%	93.8%	93.6%

V. CONCLUSION

The proposed TRIAC dimming LED driver with a variable switched capacitor was verified in an 80 W LED application. The driver is simple and compact and may thus serve as a practical solution for industrial lighting applications, such as those for streets, factories, parking garages, and emergency stairs. Contrary to SMPS LED drivers using high-frequency switches, the proposed LED driver is equipped with a TRIAC switch that serves as the main switch [7]-[24]. Hence, the proposed driver is more power-efficient, more reliable, and longer lasting than conventional drivers. LED dimming up to 81% is possible by modulating the volume resistor, which value is enough to modulate LED brightness in practical applications. LED power can be successfully regulated within 3.75% for a wide range of 190 V < V_s < 250 V. The measured power efficiency, PF, and THD were 93.8%, 0.95, and 22.5%, respectively, at V_s = 220 V. By virtue of the proposed TRIAC dimming LED driver, a long operating life, high power efficiency, and LED dimming and LED power regulation capabilities can be successfully realized.

REFERENCES

[1] J. Y. Tsao, "Solid-state lighting: lamps, chips, and materials for tomorrow," *IEEE Circuits & Devices Magazine*, Vol. 20, No. 3, pp. 28-37, May/Jun. 2004.

[2] K. Streubel, N. Linder, R. Wirth, and A. Jaeger, "High brightness AlGaInP light-emitting diodes," *IEEE J. Sel. Types Quantum Electron.*, Vol. 8, No. 2, pp. 321-332, Mar./Apr. 2002.

[3] Y. K. Cheng and K. W. E. Cheng, "General study for using LED to replace traditional lighting devices," *IEEE International Conference on Power Electronics Systems and Applications (ICPESA)*, pp. 173-177, 2006.

[4] D. A. Steigerwald, J. C. Bhat, D. Collins, R. M. Fletcher, M. O. Holcomb, M. J. Ludowise, P. S. Martin, and S. L. Rudaz, "Illumination with solid state lighting technology," *IEEE J. Sel. Topics Quantum Electron.*, pp. 310-320, Apr. 2002.

[5] M. Wendt and J.-W. Andriesse, "LEDs in real lighting applications: from niche markets to general lighting," *IEEE Industry Applications Conference*, pp. 2601-2603, 2006.

[6] S. Y. R. Hui and Y. X. Qin, "A general photo-electro-thermal theory for light emitting diode (LED) systems," *IEEE Trans. Power Electron.*, Vol. 24, No. 8, pp. 1967-1976, Aug. 2009.

[7] B. Wang, X. Ruan, K. Yao, and M. Xu, "A method of reducing the peak-to-average ratio of LED current for electrolytic capacitor-less AC–DC drivers," *IEEE Trans. Power Electron.*, Vol. 25, No. 3, pp. 592-601, Mar. 2010.

[8] S.-S. Hong, S. H. Lee, S. H. Cho, C.-W. Roh, and S. K. Han, "A new cost-effective current-balancing multi-channel LED driver for a large screen LCD backlight units," *Journal of Power Electronics*, Vol. 10, No. 4, pp. 351-356, Apr. 2010.

[9] H. Kim, and S. Kim, and K-Y. Lee, "A dual-output integrated LLC resonant controller and LED driver IC with PLL-based automatic duty control," *Journal of Power Electronics*, Vol. 12, No. 6, pp. 886-894, Nov. 2012.

[10] Y.-S. Jung and M.-G. Kim, "Time-delay effects on DC characteristics of peak current controlled power LED drivers," *Journal of Power Electronics*, Vol. 12, No. 5, pp. 715-722, Sep. 2012.

[11] X. Wu, J. Zhang, and Z. Qian, "A simple two-channel LED driver with automatic precise current sharing," *IEEE Trans. Ind. Electron.*, Vol. 58, No. 10, pp. 4783-4788, Oct. 2011.

[12] D. G. Lamar, M. Arias, A. Rodriguez, A. Fernandez, M. M. Hernando, and J. Sebastian, "Design-oriented analysis and performance evaluation of a low-cost high-brightness LED driver based on flyback power factor corrector," *IEEE Trans. Ind. Electron.*, Vol. 60, No. 7, pp. 2614-2626, Jul. 2013.

[13] Q. Hu and R. Zane, "Minimizing required energy storage in off-line LED drivers based on series-input converter modules," *IEEE Trans. Power Electron.*, Vol. 26, No. 10, pp. 2887-2895, Oct. 2011.

[14] Q. Luo, B. Zhu, W. Lu, and L. Zhou "High step-down multiple-output LED driver with the current auto-balance characteristic," *Journal of Power Electronics*, Vol. 12, No. 4, pp. 519-527, Jul. 2012.

[15] Z. Ye, F. Greenfeld, and Z. Liang, "Single-stage offline SEPIC converter with power factor correction to drive high brightness LEDs," *IEEE Applied Power Electronics Conference and Exposition (APEC),* pp. 546-553, 2009.

[16] Y. Hu, L. Huber, and M. M. Jovanovi´, "Single-stage, universal-input AC/DC LED driver with current-controlled variable PFC boost inductor," *IEEE Trans. Power Electron.*, Vol. 27, No. 3, pp. 1579-1588, Mar. 2012.

[17] H. van der Broeckl, G. Sauerlander, M. Wendt, "Power driver topologies and control schemes for LEDs," *IEEE Applied Power Electronics Conference and Exposition (APEC)*, pp. 1319-1325, 2007.

[18] J. M. Alonso, J. Viña, D. G. Vaquero, G. Martínez, and R. Osorio, "Analysis and design of the integrated double buck–boost converter as a high-power-factor driver for power-LED lamps," *IEEE Trans. Ind. Electron.*, Vol. 59, No. 4, pp. 1689-1697, Apr. 2012.

[19] S. Jung and G.-H. Cho, "Transformer coupled recycle snubber for high-efficiency offline isolated LED driver with on-chip primary-side power regulation," *IEEE Trans. Ind. Electron.*, Vol. 61, No. 12, pp. 6710-6719, Dec. 2014.

[20] J. Zhang, T. Jiang, L. Xu, and X. Wu, "Primary side constant power control scheme for LED drivers compatible with TRIAC dimmers," *Journal of Power Electronics*, Vol. 13, No. 4, pp. 609-618, Jul. 2013.

[21] S. Moon, G.-B. Koo, and G.-W. Moon, "Dimming-feedback control method for TRIAC dimmable LED drivers," *IEEE Trans. Ind. Electron.*, Vol. 62, No. 2, pp. 960-965, Aug. 2014.

[22] Y.-C. Li, "A novel control scheme of quasi-resonant valley-switching for high-power-factor AC-to-DC LED drivers," *IEEE Trans. Ind. Electron.*, Vol. 62, No. 8, pp. 4787-4794, Aug. 2015.

[23] C.-B. Park, B.-H. Choi, J.-P. Cheon, and C.-T. Rim, "Robust active LED driver with high power factor and low total harmonic distortion compatible with a rapid-start ballast," *Journal of Power Electronics*, Vol. 14, No. 2, pp. 226-236, Mar. 2014.

[24] S.-S. Hwang, W.-S. Hwang, and S.-K. Han, "Cost-effective single switch multi-channel LED driver," *Journal of Power Electronics*, Vol. 15, No. 2, pp. 319-326, Mar. 2015.

[25] S. Y. R. Hui, S. N. Li, X. H. Tao, W. Chen, and W. M. Ng, "A novel passive offline LED driver with long lifetime," *IEEE Trans. Power Electron.*, Vol. 25, No. 10, pp. 2665-2672, Oct. 2012.

[26] W. Chen, "A comparative study on the circuit topologies for offline passive light-emitting diode (LED) drivers with long lifetime & high efficiency," *IEEE Energy Conversion Congress and Exposition (ECCE)*, pp. 724-730, 2010.

[27] B. H. Lee, H. J. Kim, and C. T. Rim, "Robust passive LED driver compatible with conventional rapid-start ballast," *IEEE Trans. Power Electron.*, Vol. 26, No. 12, pp. 3694-3706, Dec. 2011.

[28] Optomind Inc., "Direct connection-type L.E.D. lighting apparatus," Korea Patent 10-2012-0094901, Aug. 29, 2012.

[29] E. S. Lee, B. H. Choi, J. P. Cheon, B. C. Kim, and C. T. Rim, "Temperature-robust LC^3 LED drivers with low THD, high efficiency and PF, and long life," *IEEE J. Emerg. Sel. Topics Power Electron.*, Vol. 3, No. 3, pp. 829-840, Jun. 2015.

[30] E. S. Lee, Y. H. Sohn, D. T. Nguyen, J. P. Cheon, and C. T. Rim, "The LED driver with TRIAC dimming control by variable switched capacitance for power regulation," *Journal of Power Electronics*, Vol. 15, No. 2, pp. 555-566, Mar. 2015.

[31] E. S. Lee, J. P. Cheon, D. T. Nguyen, and C. T. Rim, "A novel TRIAC dimming LED driver by variable switched capacitance for power regulation," *IEEE Energy Conversion Congress and Exposition (ECCE)*, pp. 2600-2605, 2014.

[32] E. S. Lee, B. H. Choi, D. T. Nguyen, and C. T. Rim, "The analysis of TRIAC dimming LED driver by variable switched capacitor for long life and high power-efficient

applications," *IEEE Power Electronics and ECCE Asia (ICPE-ECCE Asia)*, pp. 54-59, 2015.
[33] J. Huh, S. W. Lee, W. Y. Lee, G. H. Cho, and C. T. Rim, "Narrow-width inductive power transfer system for online electrical vehicles," *IEEE Trans. Power Electron.*, Vol. 26, No. 12, pp. 3666-3679, Dec. 2011.
[34] S. Lee, B. Choi, and C. T. Rim, "Dynamics characterization of the inductive power transfer system for online electric vehicles by Laplace phasor transform," *IEEE Trans. Power Electron.*, Vol. 28, No. 12, pp. 5902-5909, Dec. 2013.
[35] C. T. Rim and G. H. Cho, "Phasor transformation and its application to the DC/AC analyses of frequency/phase controlled series resonant converters (SRC)," *IEEE Trans. Power Electron.*, Vol. 5, No. 2, pp. 201-211, Apr. 1990.
[36] C. T. Rim, D. Y. Hu, and G. H. Cho, "Transformers as equivalent circuits for switches: general proofs and D-Q transformation-based analysis," *IEEE Trans. Ind. Appl.*, Vol. 26, No. 4, pp. 777-785, Jul./Aug. 1990.
[37] C. T. Rim, "Unified general phasor transformation for AC converters," *IEEE Trans. Power Electron.*, Vol. 26, No. 9, pp. 2465-2475, Sep. 2011.
[38] C. B. Park, S. W. Lee, and C. T. Rim, "Static and dynamic analyses of three-phase rectifier with LC input filter by Laplace phasor transformation," *IEEE Energy Conversion Congress and Exposition (ECCE)*, pp. 1570-1577, 2012.
[39] *IEEE Recommended Practices for Modulating Current in High-Brightness LEDs for Mitigating Health Risks to Viewers*, IEEE Std 1789-2015, 2015.
[40] ENERGY STAR program requirements for solid state lighting luminaires, Eligibility Criteria – Version 1.1, 2008.
[41] *IEC 61000-3-2 class C standard*, Limits for harmonic current emissions (equipment input current ≤ 16A per phase), 2009.

Eun-Soo Lee was born in Korea, in 1986. He received his B.S. degree in Electrical Engineering from Inha University, Incheon, Korea, in 2012, and his M.S. degree in Nuclear and Quantum Engineering from the Korea Advanced Institute of Science and Technology (KAIST), Daejeon, Korea, in 2014. Since 2014, he has been working toward his Ph.D. degree at KAIST. He has developed LED drivers and wireless power transfer systems. His current research interests include power converters, wireless power transfer systems, and LED drivers.

Bo-Hwan Choi was born in Korea, in 1988. He received his B.S. degree in Electrical Engineering from Sungkyunkwan University, Suwon, Korea, in 2011, and his Ph.D. degree in Nuclear and Quantum Engineering at Korea Advanced Institute of Science and Technology (KAIST), Daejeon, Korea, in 2016. His current research interests include power converters, wireless power transfer systems, magnetics, and energy grid applications.

Duy Tan Nguyen was born in Vietnam, in 1987. He received his B.S. degree in Electrical Engineering from the Ho Chi Minh City University of Technology, Ho Chi Minh City, Vietnam, in 2010, and his M.S. degree in Nuclear and Quantum Engineering from the Korea Advanced Institute of Science and Technology (KAIST), Daejeon, Korea, in 2016. From 2010 to 2011, he was an embedded automobile software engineer at Gate Technology, Ho Chi Minh City, Vietnam. From 2011 to 2013, he was an embedded engineer at Koda System, Hanam, Korea, where he conducted research on power measurement instruments. His current research interests include power converters, inverters, wireless power transfer systems, and LED drivers.

Byeung-Guk Choi was born in Korea in 1990. He received his B.S. degree in Mechanical Engineering from Pusan National University, Busan, Korea, in 2015. He is currently pursuing his Integrated Master's Ph.D. degree in Nuclear and Quantum Engineering at KAIST, Daejeon, Korea. His current research interests include wireless power transfer systems.

Chun-Taek Rim was born in Korea in 1963. He received his B.S. degree with Honors in Electrical Engineering from the Kumoh Institute of Technology (KIT), Korea, in 1985, and his M.S. and Ph.D. degrees in Electrical Engineering from the Korea Advanced Institute of Technology (KAIST), Korea, in 1987 and 1990, respectively.
Since 2007, he has been an associate professor of Nuclear and Quantum Engineering at KAIST. He has been developing various wireless power technologies including inductive power transfer systems for On-Line Electrical Vehicles (OLEV), and leading the Nuclear Power Electronics and Robots Lab (PEARL) at KAIST. From 1990 to 1995, he was a military officer at the Ministry of National Defense in Korea. From 1995 to 2003, he was a senior researcher at the Agency for Defense Development, Daejeon, Korea. From 1997 to 1999, he was with Astrium in Portsmouth, U.K. From 2003 to 2007, he was a senior director at the Presidential Office, Seoul, Korea. He was involved in developing Korea's first airborne and spaceborne synthetic aperture radars. His research areas include wireless electric vehicles, wireless power systems for robots, mobiles, wearables and IoT, and general unified modeling of power electronics. He has authored and coauthored 142 technical papers, has written 8 books, and holds 141 patents (awarded and pending). He has won numerous awards, including the Best Paper Award of IEEE Power Electronics Transactions in 2015 (wireless power) and three prizes awarded by the Korean government. He was the chair of the Wireless Power Committee of KIPE from 2010 to 2015, and the chair of the EV Charger Committee of KIEE since 2011, respectively. He is now an associate editor of IEEE Transactions on Power Electronics and the Journal of Emerging and Selected Topics in Power Electronics (J-ESTPE); a guest editor of the Special Issue on Wireless Power Transfer of the IEEE Transactions on Power Electronics, IEEE Transactions on Industrial Electronics, and J-ESTPE; and the general chair of the 2014 IEEE VTC-Workshop on Wireless Power (WoW), 2015 IEEE WoW, and 2016 IEEE WoW.